

# Sphere Decoding for Unique Word OFDM

Alexander Onic and Mario Huemer  
Institute of Networked and Embedded Systems  
Alpen-Adria-Universität Klagenfurt, Austria  
Email: {alexander.onic, mario.huemer}@uni-klu.ac.at

**Abstract**—The recently presented UW-OFDM (Unique Word - orthogonal frequency division multiplexing) signaling scheme [1] uses certain subcarriers in frequency domain for redundant symbols instead of data, in order to generate a zero word in the DFT (discrete Fourier transform) interval in time domain. These redundant symbols depend on the data loaded on the other carriers and thus introduce correlation. The resulting linear system model enables sophisticated detectors for data recovery. As the best known maximum likelihood detector for this case, we applied the Sphere Decoding (SD) algorithm to a single antenna UW-OFDM system and evaluated its bit error performance in AWGN (additive white Gaussian noise) and frequency selective environments. Compared to linear receivers, the SD is able to take the correlations on the redundant subcarriers optimally into account and shows an enormous gain. A reduction of the redundant energy by increasing the number of redundant subcarriers improved the bit error performance of UW-OFDM systems with linear data estimators [2] at the price of a lower bandwidth efficiency. In contrast it is found, that a receiver based on Sphere Decoding is able to optimally exploit the excess redundant energy. The SD based system therefore shows its best performance at maximum bandwidth efficiency.

## I. INTRODUCTION

The recently presented Unique Word (UW) OFDM signaling scheme [1] uses a deterministic sequence in the guard interval of an OFDM symbol, instead of the cyclic prefix, as it is used in most current OFDM applications. By putting the UW inside the DFT (discrete Fourier transform) interval in time domain the usual cyclicity of the OFDM symbol is ensured. This is achieved by loading certain subcarriers in frequency domain with redundant symbols instead of data. These redundant values depend on the data, and thus introduce correlation.

For the classic and well known cyclic prefix OFDM, equalizers following the zero forcing (ZF) principle are optimal. On the contrary, due to the introduced correlations, UW-OFDM allows for much more sophisticated data estimation strategies.

As shown in [1], the LMMSE (linear minimum mean square error) data estimator uses some information from the redundant carriers beneficially, in order to improve the MSE. However, the fact that correlations are introduced as part of the transmit process allows the use of many more receiver

structures. As we show in Sec. II, the system model can be interpreted as a MIMO channel, which enables the application of all the receivers known from the MIMO (multiple input multiple output) world to be used with single antenna UW-OFDM systems.

The paper is organized as follows: The UW-OFDM system description will be presented in Sec. II. Interpreted as a MIMO channel, the best known receiver for this is a maximum likelihood sequence estimator (MLSE). An efficient implementation is the Sphere Decoder, whose realization for a single antenna Unique Word OFDM system will be discussed in Sec. III. In order to quantify the gain of Sphere Decoding in comparison to other data estimation strategies, we will show simulation results of a Unique Word OFDM system in a multi-path as well as AWGN (additive white Gaussian noise) environment in Sec. IV. In Sec. V we conclude this work.

## II. UNIQUE WORD OFDM SYSTEM MODEL

We briefly review the approach of introducing unique words in OFDM. For further details see [1]. Let  $\mathbf{x}_u$  be a predefined sequence of length  $N_u$ , which we call the Unique Word. This Unique Word shall form the tail of the OFDM time domain symbol vector. Hence, the time domain symbol vector, as the result of the length  $N$  IDFT (inverse DFT), consists of two parts and is of the form  $[\mathbf{x}_d^T \ \mathbf{x}_u^T]^T \in \mathbb{C}^{N \times 1}$ , whereas only  $\mathbf{x}_d \in \mathbb{C}^{(N-N_u) \times 1}$  is random and affected by the data. It turned out that, in order to generate the OFDM symbol, it is advantageous to generate an OFDM symbol

$$\mathbf{x} = \begin{bmatrix} \mathbf{x}_d \\ \mathbf{0} \end{bmatrix} \quad (1)$$

with a zero UW in a first step, and to add the desired UW to determine the transmit symbol

$$\mathbf{x}' = \mathbf{x} + \begin{bmatrix} \mathbf{0} \\ \mathbf{x}_u \end{bmatrix}, \quad (2)$$

in a second step [3]. Just as in conventional OFDM, the OFDM symbol is specified by the QAM data symbols in frequency domain. As we intend a certain number of zero symbols according to (1) in a part of the IDFT output, we have to load at least the same number of subcarriers in frequency domain with appropriate values. We want to name these *redundant* subcarriers, as they are loaded with values depending on the data  $\tilde{\mathbf{d}} \in \mathbb{C}^{N_d \times 1}$ . The redundant values are as well gathered in

a vector  $\tilde{\mathbf{r}} \in \mathbb{C}^{N_r \times 1}$ . We denote the frequency domain OFDM symbol vector as

$$\tilde{\mathbf{x}} = \mathbf{P} \begin{bmatrix} \tilde{\mathbf{d}} \\ \tilde{\mathbf{r}} \end{bmatrix}, \quad \tilde{\mathbf{x}} \in \mathbb{C}^{N \times 1}, \quad (3)$$

utilizing a permutation matrix  $\mathbf{P} \in \{0, 1\}^{N \times N}$  to place the data and redundant values to their dedicated subcarriers. In contrast to [1], [3], [4], we assemble the OFDM symbols without introducing zero subcarriers in frequency domain at the band edges and at the DC carrier.

Employing the  $N$  point DFT matrix  $\mathbf{F}_N$  with its element in the  $k$ -th row and the  $l$ -th column  $[\mathbf{F}_N]_{kl} = e^{-j\frac{2\pi}{N}kl}$ , the time-frequency relation of the OFDM symbol can now be written as

$$\mathbf{F}_N^{-1} \mathbf{P} \begin{bmatrix} \tilde{\mathbf{d}} \\ \tilde{\mathbf{r}} \end{bmatrix} = \begin{bmatrix} \mathbf{x}_d \\ \mathbf{0} \end{bmatrix}. \quad (4)$$

With

$$\mathbf{M} = \mathbf{F}_N^{-1} \mathbf{P} = \begin{bmatrix} \mathbf{M}_{11} & \mathbf{M}_{12} \\ \mathbf{M}_{21} & \mathbf{M}_{22} \end{bmatrix}, \quad (5)$$

where  $\mathbf{M}_{kl}$  are appropriately sized sub-matrices, it follows that  $\mathbf{M}_{21}\tilde{\mathbf{d}} + \mathbf{M}_{22}\tilde{\mathbf{r}} = \mathbf{0}$ , and hence  $\tilde{\mathbf{r}} = -\mathbf{M}_{22}^{-1}\mathbf{M}_{21}\tilde{\mathbf{d}}$ . With the matrix

$$\mathbf{T} = -\mathbf{M}_{22}^{-1}\mathbf{M}_{21}, \quad \mathbf{T} \in \mathbb{C}^{N_r \times N_d}, \quad (6)$$

the vector of redundant subcarrier symbols can thus be determined by the linear mapping

$$\tilde{\mathbf{r}} = \mathbf{T}\tilde{\mathbf{d}}. \quad (7)$$

Furthermore, with the definition of

$$\mathbf{G} = \mathbf{P} \begin{bmatrix} \mathbf{I} \\ \mathbf{T} \end{bmatrix}, \quad \mathbf{G} \in \mathbb{C}^{N \times N_d}, \quad (8)$$

the transmit symbol can now be written as

$$\mathbf{x}' = \mathbf{F}_N^{-1} \mathbf{G}\tilde{\mathbf{d}} + \begin{bmatrix} \mathbf{0} \\ \mathbf{x}_u \end{bmatrix}, \quad (9)$$

and with the UW influence in frequency domain  $\tilde{\mathbf{x}}_u = \mathbf{F}_N [\mathbf{0}^T \quad \mathbf{x}_u^T]^T$  we can also write

$$\mathbf{x}' = \mathbf{F}_N^{-1} (\mathbf{G}\tilde{\mathbf{d}} + \tilde{\mathbf{x}}_u). \quad (10)$$

The construction of  $\mathbf{T}$  highly depends on the choice of  $\mathbf{P}$ . In [1] it is suggested to choose  $\mathbf{P}$  by a minimization of the symbol energy  $E_{\mathbf{x}'} = \mathbb{E} \{ \mathbf{x}'^H \mathbf{x}' \}$  which leads to the optimization problem

$$\mathbf{P} = \operatorname{argmin} \left\{ \operatorname{tr}(\mathbf{T}\mathbf{T}^H) \right\}, \quad (11)$$

where  $\mathbf{T}$  is derived from (6) and (5).

While usually the number of redundant subcarriers is chosen to the length of the Unique Word  $N_r = N_u$ , in [2] also the case  $N_r > N_u$  is considered. Adapting the dimensions of the sub-matrices in (5), the solution to (6) still exists. It was shown, that the matrix inverse  $M_{22}^{-1}$  in (6) becomes a pseudo inverse  $M_{22}^+ = (M_{22}^H M_{22})^{-1} M_{22}^H$ , while the remaining process stays the same. When determining (11) with this new system setup,

even lower OFDM symbol energies and likewise better BER performances can be achieved with an LMMSE receiver [2]. This gain comes of course with a loss of bandwidth efficiency, as less data is transmitted in one OFDM symbol.

The propagation of the OFDM symbol, assembled according to (10), through a multi-path channel is modeled using a cyclic convolution matrix  $\mathbf{H}_c$  and a noise vector  $\mathbf{n}$  with the covariance matrix  $\mathbf{C}_{nn} = \sigma_n^2 \mathbf{I}$ . After applying the DFT in the receiver, the frequency domain receive vector can be formulated as

$$\begin{aligned} \tilde{\mathbf{y}}_r &= \mathbf{F}_N \mathbf{H}_c \mathbf{x}' + \underbrace{\mathbf{F}_N \mathbf{n}}_{\tilde{\mathbf{v}}} \\ &= \mathbf{F}_N \mathbf{H}_c \mathbf{F}_N^{-1} (\mathbf{G}\tilde{\mathbf{d}} + \tilde{\mathbf{x}}_u) + \tilde{\mathbf{v}}. \end{aligned} \quad (12)$$

The matrix  $\tilde{\mathbf{H}} = \mathbf{F}_N \mathbf{H}_c \mathbf{F}_N^{-1}$  is diagonal and contains the sampled channel frequency response on its main diagonal. As a first receiver processing step we subtract the UW influence to obtain the symbol  $\tilde{\mathbf{y}} = \tilde{\mathbf{y}}_r - \tilde{\mathbf{H}}\tilde{\mathbf{x}}_u$  and arrive at the form of a linear model

$$\tilde{\mathbf{y}} = \tilde{\mathbf{H}}\mathbf{G}\tilde{\mathbf{d}} + \tilde{\mathbf{v}}. \quad (14)$$

The channel propagation matrix  $\tilde{\mathbf{H}}\mathbf{G}$  of size  $N \times N_d$  can be interpreted as the propagation matrix of a complex MIMO channel, although we only modeled a single antenna system: The  $N_d$  data subcarrier positions in the receive vector are simply the data values sent and disturbed by the channel. The  $N_r$  redundant subcarrier positions depend on all data symbols, in a way described by the matrix  $\mathbf{T}$ . This altogether allows us to treat the UW-OFDM system as a MIMO system with  $N_d$  transmit and  $N$  receive antennas, and to use any MIMO detection method to recover the data.

### III. SPHERE DECODING

The best decoding results recovering  $\tilde{\mathbf{d}}$  from (14) are achieved by a Maximum Likelihood Sequence Estimation on each OFDM symbol. In the introduced terminology of the linear system model this translates to the minimization of the distance of all possible OFDM symbols after channel propagation to the received vector:

$$\hat{\tilde{\mathbf{d}}} = \operatorname{argmin}_{\tilde{\mathbf{d}} \in \mathcal{A}^{N_d}} \|\tilde{\mathbf{H}}\mathbf{G}\tilde{\mathbf{d}} - \tilde{\mathbf{y}}\|_2^2. \quad (15)$$

In theory, *every* possible noise-free receive vector  $\tilde{\mathbf{H}}\mathbf{G}\tilde{\mathbf{d}}$ , with the vector  $\tilde{\mathbf{d}}$  containing  $N_d$  values from the chosen QAM alphabet  $\mathcal{A}$ , needs to be examined for its Euclidean norm, which is impossible for practical UW-OFDM systems. E.g. for one of the simulation modes used in this work (see Sec. IV-A), there exist  $|\mathcal{A}|^{N_d} = 16^{48} > 6 \cdot 10^{57}$  possible different OFDM symbols.

To allow for MLSE within a practical amount of computational time, Sphere Decoding is a well known method originating from MIMO decoding. For this work, we applied the Sphere Decoding algorithm on a single antenna system in a multi-path environment.

First, a QR decomposition of the transmission matrix

$$\tilde{\mathbf{H}}\mathbf{G} = \mathbf{Q} \begin{bmatrix} \mathbf{R} \\ \mathbf{0} \end{bmatrix} \quad (16)$$

enables the required simplifications, where  $\mathbf{Q} \in \mathbb{C}^{(N \times N)}$  is a unitary matrix and  $\mathbf{R} \in \mathbb{C}^{N_d \times N_d}$  is upper triangular.

Partitioning  $\mathbf{Q} = [\mathbf{Q}_1 \quad \mathbf{Q}_2]$ , with  $\mathbf{Q}_1$  of size  $(N \times N_d)$  and  $\mathbf{Q}_2$  of size  $(N \times N_u)$ , we can elaborate the Euclidean distance in (15) as

$$\begin{aligned} \|\tilde{\mathbf{H}}\mathbf{G}\tilde{\mathbf{d}} - \tilde{\mathbf{y}}\|_2^2 &= \left\| \mathbf{Q} \begin{bmatrix} \mathbf{R} \\ \mathbf{0} \end{bmatrix} \tilde{\mathbf{d}} - \tilde{\mathbf{y}} \right\|_2^2 \\ &= \left\| \mathbf{Q}^H \mathbf{Q} \begin{bmatrix} \mathbf{R} \\ \mathbf{0} \end{bmatrix} \tilde{\mathbf{d}} - \mathbf{Q}^H \tilde{\mathbf{y}} \right\|_2^2 \\ &= \left\| \begin{bmatrix} \mathbf{R} \\ \mathbf{0} \end{bmatrix} \tilde{\mathbf{d}} - \begin{bmatrix} \mathbf{Q}_1^H \\ \mathbf{Q}_2^H \end{bmatrix} \tilde{\mathbf{y}} \right\|_2^2 \\ &= \|\mathbf{R}\tilde{\mathbf{d}} - \mathbf{Q}_1^H \tilde{\mathbf{y}}\|_2^2 + \|\mathbf{Q}_2^H \tilde{\mathbf{y}}\|_2^2. \end{aligned} \quad (17)$$

As the second term is independent of  $\tilde{\mathbf{d}}$ , the minimization problem (15) becomes

$$\hat{\tilde{\mathbf{d}}} = \underset{\tilde{\mathbf{d}} \in \mathcal{A}^{N_d}}{\operatorname{argmin}} \left\| \mathbf{R}\tilde{\mathbf{d}} - \mathbf{Q}_1^H \tilde{\mathbf{y}} \right\|_2^2. \quad (18)$$

With the description in (18), one of the many Sphere Decoding algorithms can be applied. For this work we used the algorithm, following the Schnorr-Euchner strategy, introduced in [5]. Anyway, we had to adapt their algorithm DECODE in order to handle the finite set  $\mathcal{A}$  of complex QAM symbols, instead of an infinite real lattice and to fit to our notation using column vectors.

The run-time complexity of the SD is known to be able to get out of hand in certain conditions. For practical systems the complexity needs to be limited, which can be achieved by several techniques, e.g. [6]. For this work we focus on the possibilities of Sphere Decoding for UW-OFDM, but implemented a reasonable high bound on the maximum number of node visits per OFDM symbol, though.

#### IV. SIMULATION RESULTS

##### A. Simulation Setup

A block diagram of the system setup used in this work for simulation is shown in Fig. 1. After the QAM mapping, the OFDM symbol is assembled in frequency domain, transformed and supplied with the UW, according to (9), resulting in the time domain signal  $\mathbf{x}'$  to be transmitted. As UW we used the zero word for our simulations.

Furthermore, we used a system with the parameters shown in Tab. I. The DFT-length as well as the Unique Word length are chosen to meet the DFT and the length of the guard interval specified in IEEE 802.11a [7].

As we used two modes for the subcarrier allocation with different  $N_d$  and  $N_r$ , we had to find an optimum  $\mathbf{P}$  for each of them using (11). The indices of the redundant subcarriers used, are listed in Tab. II. These modes will be named  $r^{(16)}$  and  $r^{(32)}$ , in order to identify the  $N_r = 16$  and 32 modes. It is

worth mentioning, that both modes show an optimum, when using an equidistant distribution of the redundant subcarriers throughout the spectrum. In Tab. II we also noted the energy per bit values  $E_b$ , as they result from determining the OFDM symbol energies  $E_{\mathbf{x}'}$  according to [3], using a normalized 16-QAM constellation. In [3] it is also shown, that the OFDM symbol energy can be decomposed to  $E_{\mathbf{x}'} = E_{\tilde{\mathbf{d}}} + E_{\tilde{\mathbf{r}}}$ , where  $E_{\tilde{\mathbf{d}}}$  corresponds to the data and  $E_{\tilde{\mathbf{r}}}$  to the redundant values. The relation between these two energies is also shown in Tab. II.

From this relation we see the noteworthy property, that the energy spent for all redundant subcarriers in relation to the overall OFDM symbol energy *decreases*, even if the number of redundant subcarriers is increased, enabling the reduction of the energy per bit  $E_b$ .

We compare the Sphere Decoding (SD) performance with two linear data estimation schemes. The first data estimator is a simple channel inversion estimator (CI), that could be seen as the equivalent of the zero forcing receiver of conventional OFDM using cyclic prefixes:

$$\mathbf{E}_{\text{CI}} = [\mathbf{I} \quad \mathbf{0}] \mathbf{P}^T \tilde{\mathbf{H}}^{-1} \quad (19)$$

This is an estimator with very low complexity, since the channel inversion  $\tilde{\mathbf{H}}^{-1}$  corresponds to a simple division of the diagonal elements. On the other hand it completely ignores the information available on the redundant carriers after the channel inversion step.

The second data estimator is the LMMSE estimator derived for UW-OFDM in former publications, e.g. [1], [4]:

$$\mathbf{E}_{\text{LMMSE}} = \left( \mathbf{G}^H \tilde{\mathbf{H}}^H \tilde{\mathbf{H}} \mathbf{G} + \frac{N\sigma_n^2}{\sigma_d^2} \mathbf{I} \right)^{-1} \mathbf{G}^H \tilde{\mathbf{H}}^H \quad (20)$$

Of some low extent, this estimator considers the redundant information, which also increases the computational complexity to determine  $\mathbf{E}_{\text{LMMSE}}$ , compared to  $\mathbf{E}_{\text{CI}}$ .

##### B. Simulation Results in the AWGN channel

The AWGN channel should allow us to observe some trends of the used transmission modes and detection strategies, as the channel frequency response does not prefer or penalize certain subcarrier settings.

TABLE I  
PARAMETERS OF THE INVESTIGATED UW-OFDM SYSTEM

Modulation scheme		16-QAM
DFT length	$N$	64
No. of data (redundant) subcarriers	$N_d$ ( $N_r$ )	48 (16), 32 (32)
Unique Word	$\mathbf{x}_u$	$\mathbf{0}^{(N_u \times 1)}$

TABLE II  
REDUNDANT SUBCARRIER MODES USED FOR THE SIMULATIONS AND THEIR ENERGY PROPERTIES

$N_r$	Set of subcarrier indices	$E_b$	$E_{\tilde{\mathbf{r}}}/E_{\mathbf{x}'}$
16	{1, 5, 9, 13, ..., 57, 61}	$7.81 \cdot 10^{-3}$	1/2
32	{1, 3, 5, 7, ..., 61, 63}	$5.86 \cdot 10^{-3}$	1/3

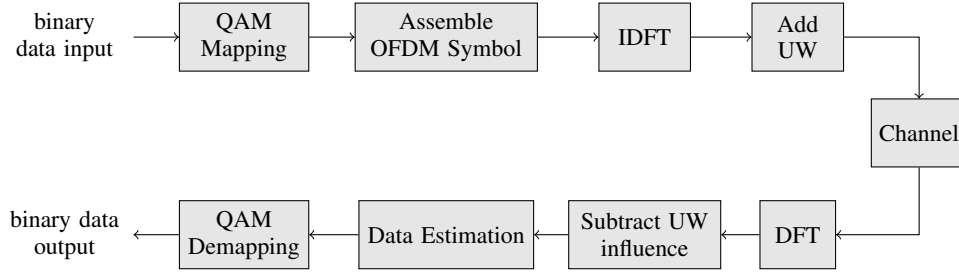


Fig. 1. Block diagram of the transceiver system used for simulation

From the bit energies  $E_b$  in Tab. II we are able to predict how the modes compare in case of the CI data estimator, as it doesn't utilize the redundant subcarriers. Relating the bit energies of the modes

$$\frac{E_b^{(16)}}{E_b^{(32)}} = 1.33 \triangleq 1.25 \text{ dB},$$

we can expect a 1.25 dB gain of  $r^{(32)}$  compared to  $r^{(16)}$ .

In Fig. 2 the bit error rate is plotted over the  $E_b/N_0$  ratio for our modes (different colors) and with the introduced data estimators (different markers). Judging from these results, the previous valuation is met by the CI estimator (square) and also approximately by the LMMSE (cross) estimator.

However, this gain is not transferred to the results when doing Sphere Decoding. Spending more subcarriers for redundancy does not yield a better bit error performance here, the modes  $r^{(16)}$  and  $r^{(32)}$  achieve almost the same bit error rates. This leads to the conclusion that the Sphere Decoder is able to exploit the entire information present on the redundant subcarriers. All energy spent, regardless of its use for data or redundant subcarriers, can be utilized beneficially for the decoding process. In contrast, the LMMSE estimator shows only very limited capabilities of processing the redundancies properly.

### C. Simulation Results in Multi-path Channels

In a frequency selective environment, the bit error performance depends not only on the OFDM symbol energies  $E_{x'}$  resulting from the choice of redundant subcarrier indices, but also strongly on the match of the characteristics of the transmission channel's frequency response with the positions of data and redundant subcarriers. For the CI data estimator a high subcarrier attenuation only has an impact, if this particular subcarrier is used for data. If this subcarrier switched its purpose to act as redundant subcarrier, the BER would improve — changing  $E_{x'}$  though.

For simulations we use two different channel snapshots. Each channel impulse response has a total duration not exceeding the guard interval. Their frequency responses are shown in Fig. 3. Channel A does not show any deep fading holes, whereas channel B features two spectral notches within the system bandwidth, both on data subcarrier positions for both modes used.

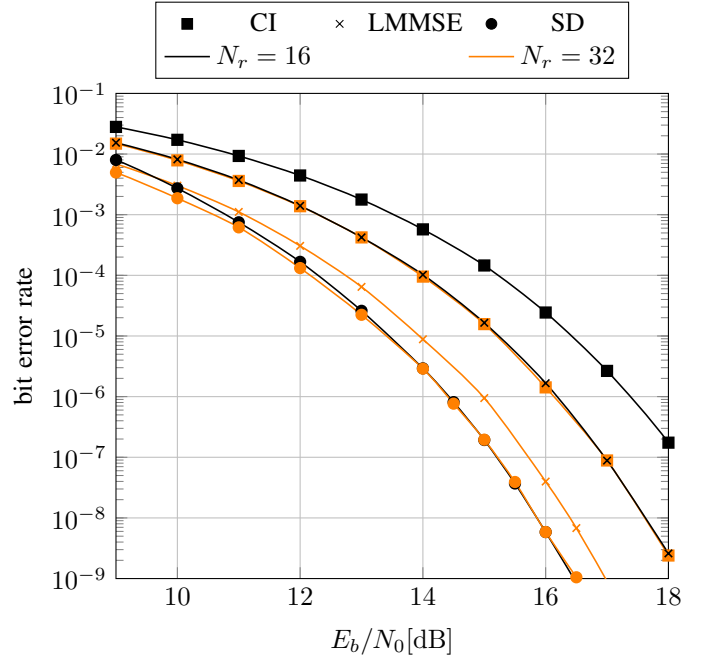


Fig. 2. BER performance in AWGN channel

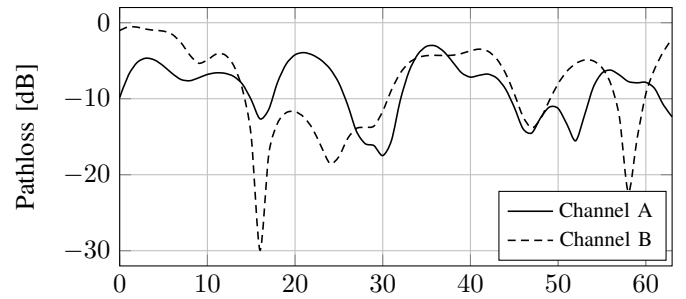


Fig. 3. Frequency responses of indoor multi-path channel snapshots

Examining the BER results for channel A in Fig. 4 yields similar results to those in the AWGN channel. Approximately the same gain of  $r^{(32)}$  compared to  $r^{(16)}$  predicted before, can be found for the CI data estimator. On the other hand, the LMMSE yields with up to 1.8 dB an even stronger advantage of the  $r^{(32)}$  mode. The SD repeats the behavior observed for the AWGN channel before. With SD however, the plot shows

a crossover point at a BER of  $10^{-3}$ , from which on the  $r^{(16)}$  mode performs better than  $r^{(32)}$ , with increasing  $E_b/N_0$ .

The same observations can be made for channel B, whose BER plots are shown in Fig. 5. The deep spectral notches of its frequency response of course have a huge impact on the performance of the CI data estimator. The methods, which incorporate the redundancy information perform almost as good as in channel A. The crossover point of the SD is again at a BER of  $10^{-3}$ .

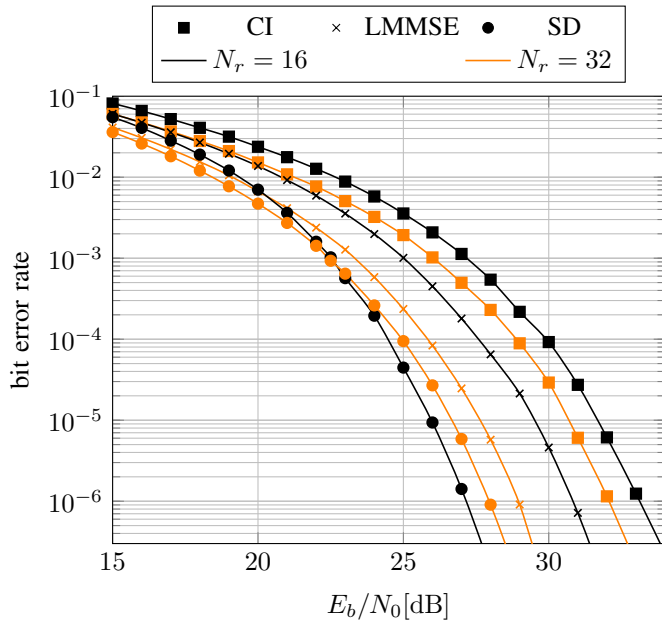


Fig. 4. BER performance in channel A

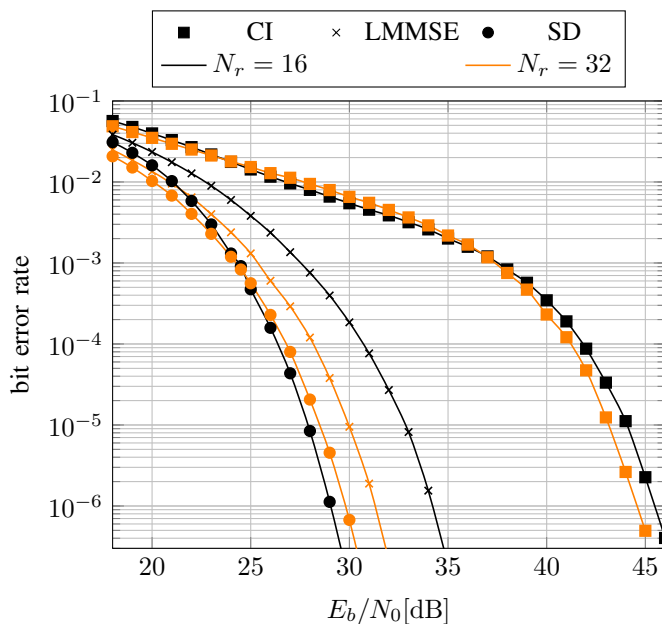


Fig. 5. BER performance in channel B

## V. CONCLUSION

The distinct system structure of the UW-OFDM signaling scheme allows for all the detection strategies known for MIMO channels, even though considering only a single antenna system. We implemented the Sphere Decoding algorithm for UW-OFDM systems and compared its bit error performance with linear receivers. For linear data estimation we considered the LMMSE estimator and the channel inversion estimator, which completely ignores the redundancy introduced by UW-OFDM. The performance was investigated using different modes, altering data and redundant subcarrier configurations.

We verified a huge gain in performance of the Sphere Decoder, as it takes the correlations on the redundant subcarriers optimally into account. However, it can be seen that decreasing the redundant energy by spending more redundant subcarriers, which improved the BER behavior for linear data estimators, is not worthwhile for the SD. The use of more subcarriers for redundant symbols does not yield a better bit error performance for the Sphere Decoder.

We conclude, that for the SD based system it is optimal to choose the minimum number of redundant subcarriers. Thus, the SD shows its best performance at maximum bandwidth efficiency.

## REFERENCES

- [1] M. Huemer, C. Hofbauer, and J. Huber, "The Potential of Unique Words in OFDM," in *Proceedings of the 15th International OFDM Workshop*, Hamburg, Sep. 2010, pp. 140–144.
- [2] C. Hofbauer, M. Huemer, and J. B. Huber, "On the Impact of Redundant Subcarrier Energy Optimization in UW-OFDM," in *4th International Conference on Signal Processing and Communication Systems (ICSPCS)*, Dec. 2010, pp. 1–6.
- [3] A. Onic and M. Huemer, "Direct vs. Two-Step Approach for Unique Word Generation in UW-OFDM," in *Proceedings of the 15th International OFDM Workshop*, Hamburg, Sep. 2010, pp. 145–149.
- [4] C. Hofbauer, M. Huemer, and J. Huber, "Coded OFDM by Unique Word Prefix," in *IEEE International Conference on Communication Systems (ICCS)*, Nov. 2010, pp. 426–430.
- [5] E. Agrell, T. Eriksson, A. Vardy, and K. Zeger, "Closest Point Search in Lattices," *IEEE Transactions on Information Theory*, vol. 48, no. 8, pp. 2201–2214, Aug. 2002.
- [6] A. Burg, M. Borgmann, M. Wenk, C. Studer, and H. Bölcskei, "Advanced Receiver Algorithms for MIMO Wireless Communications," in *Design, Automation and Test in Europe, DATE '06*, vol. 1, Mar. 2006, p. 6.
- [7] *IEEE Std 802.11a-1999, Part 11: Wireless LAN Medium Access Control (MAC) and Physical Layer (PHY) specifications: High-Speed Physical Layer in the 5 GHz Band*, IEEE Std., 1999.